# Circularly polarized molecular high-order harmonic generation in $H_2^+$ with intense laser pulses and static fields

Kai-Jun Yuan and André D. Bandrauk*

*Laboratoire de Chimie Théorique, Faculté des Sciences, Université de Sherbrooke, Sherbrooke, Québec, Canada J1K 2R1*

(Received 3 May 2011; published 30 June 2011)

Molecular high-order harmonic generation (MHOHG) by a combined intense circularly polarized laser pulse and static electric field has been studied from the appropriate time-dependent Schrödinger equation (TDSE) for the $H_2^+$ molecular ion. It is found that for a particular static field strength derived from a classical model, efficient MHOHG spectra are obtained with maximum energy $I_p + 9.05U_p$, where $I_p$ is the ionization potential and $U_p = E_0^2/4m_e\omega_0^2$ is the ponderomotive energy at amplitude $E_0$ and frequency $\omega_0$ of the circularly polarized laser pulse. The static field controls recollision of the electron with *parent* ions and is confirmed by numerical solutions of the $H_2^+$ TDSE at equilibrium. To produce circularly polarized MHOHG spectra, a combination of an elliptically polarized pulse and a static electric field is found to be most efficient. A time-frequency analysis obtained via Gabor transforms is employed to identify electron recollision times responsible for the generation of these high-order harmonics. It is found that only single recollision trajectories contribute to the circularly polarized harmonics, thus generating new sources for high-frequency circularly polarized attosecond pulses.

DOI: 10.1103/PhysRevA.83.063422 PACS number(s): 33.80.Rv, 42.65.Ky

## I. INTRODUCTION

Taking advantage of the advances in the synthesis and characterization of phase stabilized ultrashort intense laser pulses [1,2], a large number of highly nonlinear nonperturbative response electron dynamics has been investigated, such as high-order harmonic generation (HHG), above threshold ionization (ATI) and laser induced electron diffraction in atomic and molecular systems [3–5]. One of the fundamental concepts of intense laser field atomic or molecular interaction has been the rescattering model in the presence of intense linearly polarized light [6]. Thus, following tunneling ionization, the electron remains "controlled" by the laser field, returning to the parent ion after a phase (sign) change of the electric field. This simple classical model of laser induced electron recollision with the parent ion has led to the development of a consistent theory of HHG in atoms [7] and molecular high-order harmonic generation (MHOHG) [4] with a recollision maximum energy law $N_m\hbar\omega_0 = I_p + 3.17U_p$, where $I_p$ is the ionization energy, and $U_p = E_0^2/4m_e\omega_0^2$ is the ponderomotive energy with electric field amplitude $E_0$ and frequency $\omega_0$. On the other hand, the returning free electron may also elastically scatter with its parent ion resulting in ATI. The corresponding recollision energy and recollision time also satisfy simple classical laws [6,8]. Two-color linearly polarized excitation schemes have furthermore shown control of the recolliding electron, including preionization where nonzero initial velocity [8] instead of the zero initial velocity of the tunneling model [6], can be used to explore new possibilities for control of the harmonic generation process. For stretched (extended) beyond equilibrium internuclear distance molecules, a possibility of extending harmonic orders or energies in MHOHG by collision with neighboring ions results in maximum kinetic energy $I_p + 8U_p$ [9–13], beyond the linearly polarized light recollision maximum energy $N_m\hbar\omega_0 = I_p + 3.17U_p$ [6–8]. In a circularly polarized bichromatic ultrashort intense laser pulse, we have also shown that maximum elliptically polarized harmonic energies of $I_p+13.5U_p$ can be generated at particular internuclear distances and relative pulse carrier envelope phase (CEP) [14].

Much progress in the investigations of the effect of static electric fields on atomic and molecular HHG spectra has been reported previously [15–20]. In particular, Milošević and Starace showed that a high-energy plateau for scattered x-ray photons was induced in a combined linearly polarized laser and static field, thus predicting an increase of the scattered x-ray energies [21] and additional plateau structure [22]. In the presence of a static field perpendicular to the linearly polarized laser field, multiple atomic HHG can be induced [23]. More recently, a far IR low-frequency chirped linearly polarized laser and static field has been used to extend HHG cutoff, up to a maximum energy $(I_p + 42U_p)$ in the one-dimensional atomic H [24]. However, most of the studies have so far focused on the effects of static fields on the atomic HHG spectra in linearly polarized laser pulses and the generation of linearly polarized atomic and molecular HHG spectra.

Since a circularly polarized laser pulse drives the ionized electron away from the parent ion and thus suppresses recollision, one, in general, can not get HHG spectra except in certain cases of double ionization [25]. Here, we present theoretical studies and results of numerical simulations to produce circularly polarized MHOHG spectra by an intense elliptical polarized laser pulse in combination with a static electric field. In previous work, we provided a method for the generation of single attosecond (asec) laser pulses from a circularly polarized MHOHG with an extended (large internuclear distances) asymmetric molecular ion $HHe^{++}$ [14]. In the present work, we show that circularly polarized MHOHG spectra can be obtained by an elliptically polarized laser and static electric field at the equilibrium internuclear distance $R_e$ of the molecular ion $H_2^+$. We first derive the electron response from classical equations and then solve the corresponding time-dependent Schrödinger equation (TDSE) for a prealigned $H_2^+$ molecular ion and show that the MHOHG spectra exhibit

*andre.bandrauk@usherbrooke.ca

 

a plateau with maximum harmonic energy $I_p+9.05U_p$ due to recollision of the ionized electron with its *parent* ion. We define the ponderomotive energy $U_p = E_0^2/4m_e\omega_0^2$, where $E_0$ is the maximum amplitude of the circularly polarized laser pulse. In order to produce circularly polarized MHOHG, we derive the conditions for such a process by an elliptically polarized laser and static electric field.

The paper is arranged as follows: in Sec. II, we present the theoretical model of electron motion and recollision in a circularly polarized laser field with an oriented static electric field based on a classical model. The computation methods are briefly described in Sec. III. The numerical results obtained by time-dependent quantum electron wave-packet calculations from the corresponding TDSE for a prealigned $H_2^+$ are presented and discussed in Sec. IV. Finally, we summarize our findings in Sec. V. We use atomic units (a.u.) $e = \hbar = m_e = 1$ throughout unless otherwise noted, so that $U_p = E_0^2/4\omega_0^2$ a.u..

## II. THEORETICAL MODEL

We first derive the electron motion in the presence of a circularly polarized laser and static electric field based on a classical model. A circularly polarized laser pulse of maximum amplitude $E_0$, corresponding to intensity $I_0 = c\varepsilon_0 E_0^2/2$ and frequency $\omega_0$, is defined as

$$E_x(t) = E_0\cos(\omega_0 t+\phi), E_y(t) = E_0\sin(\omega_0 t+\phi). \quad (1)$$

In general, in the circularly polarized laser field, no recollision of the electron with parent ions occurs. In combination with a static electric field $E_s = -s_0$ along the $y$ direction, the classical field equations of motion [$\ddot{x}(t) = -E_x(t)$, $\ddot{y}(t) = -E_y(t) - E_s(t)$] give the time-dependent laser induced velocities

$$\begin{aligned}\dot{x}(t) &= -\frac{E_0}{\omega_0}[\sin(\omega_0 t+\phi)-\sin\phi],\\ \dot{y}(t) &= -\frac{E_0}{\omega_0}[\cos\phi-\cos(\omega_0 t-\phi)]+s_0 t,\end{aligned} \quad (2)$$

where we impose the initial zero velocity conditions, $\dot{x}(0) = \dot{y}(0) = 0$, as the first step in tunneling ionization [6,8]. The resulting electron time-dependent displacements are

$$\begin{aligned}x(t) &= -\frac{E_0}{\omega_0^2}[\cos\phi-\cos(\omega_0 t+\phi)-\omega_0 t\sin\phi],\\ y(t) &= -\frac{E_0}{\omega_0^2}[\omega_0 t\cos\phi+\sin\phi-\sin(\omega_0 t+\phi)]+\frac{1}{2}s_0 t^2.\end{aligned} \quad (3)$$

Imposing the recollision conditions with the parent ion, the field induced displacements are $x(t_c) = y(t_c) = 0$ in Eq. (3), for which Fig. 1 displays the kinetic energies $K_{ex}(t_c) = \dot{x}(t_c)/2$, $K_{ey}(t_c) = \dot{y}(t_c)/2$, and total $K_e(t_c) = K_{ex}(t_c)+K_{ey}(t_c)$ in Eq. (2) with respect to the CEP $\phi$ and $\omega_0 t_c$ at recollision time $t_c$. Note that from Eqs. (2) and (3) in the circularly polarized laser and static field, recollision of the electron with its parent ion takes place once at each optical cycle, differing from the case of the linearly polarized laser pulse in which recollision occurs at each half cycle, due to the asymmetry of the field in the $y$ direction. Maximizing the total kinetic energy with respect to the CEP $\phi$ and collision phase $\omega_0 t_c$ [14] with value $K_e(t_c) = 9.05U_p$ gives $\phi = (2n+0.016)\pi$ and $\omega_0 t_c = (2n+1.742)\pi$, $n = 0,1,2,\ldots$, where the

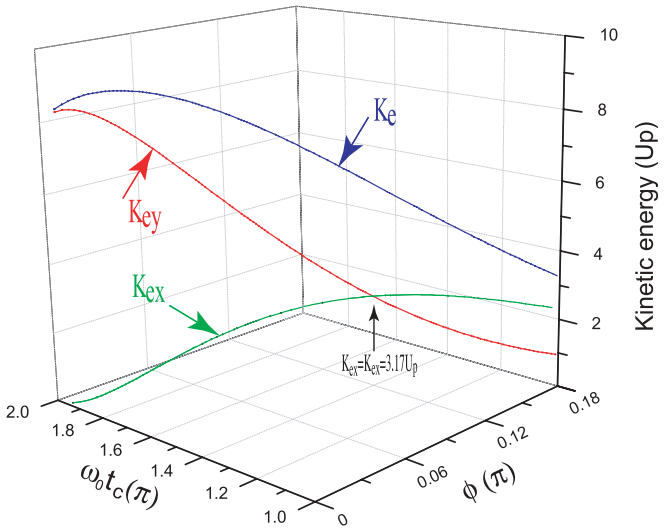


FIG. 1. (Color online)Kinetic energies $K_{ex}$, $K_{ey}$, and total $K_e = K_{ex}+K_{ey}$ as functions of the CEP $\phi$ and recollision phase $\omega_0 t_c$ for electron recollision with the parent ion where $x(t_c) = y(t_c) = 0$ [Eq. (3)].

ponderomotive energy of the electron is $U_p = E_0^2/4\omega_0^2$, with $K_{ex}(t_c) = 1.1U_p$ and $K_{ey}(t_c) = 7.95U_p$. The corresponding static electric field strength is $s_0 = 0.414E_0$. However, one notes that the kinetic energy of the electron in the $y$ direction is larger than that in the $x$ direction, $K_{ey}(t_c) = 7.95K_{ey}$. As numerical results show below, more photons will contribute to the $y$ component in the harmonic spectra.

In order to obtain equal signal amplitudes in both $x$ and $y$ components, we impose the same kinetic energies $K_{ex}(t_c)$ and $K_{ey}(t_c)$ of the electron acquired at recollision time $t_c$. From Eqs. (2) and (3) and Fig. 1, one then gets the corresponding optimal values: the static field strength $s_0 = 0.617E_0$, the CEP $\phi = (2n+0.1)\pi$, and the recollision time $t_c = (2n+1.3)\pi/\omega_0$, leading to the total kinetic energy $K_e(t_c) = 6.34U_p$, with $K_{ex}(t_c) = \dot{x}^2(t_c)/2 = 3.17U_p$ and $K_{ey}(t_c) = \dot{y}^2(t_c)/2 = 3.17U_p$. We have thus achieved in duplicating the standard atomic recollision energy in both directions.

## III. COMPUTATIONAL METHOD

We consider next the two-dimensional (2D) $H_2^+$ molecular ion at a fixed internuclear separation $R$ (Born-Oppenheimer approximation), interacting with the combination of a circularly polarized laser pulse $\mathbf{E}_{lp}(t)$ and a static electric field $\mathbf{E}_s(t)$. The corresponding 2D (plane) TDSE

$$i\frac{\partial}{\partial t}\Psi(\mathbf{r},t) = H(\mathbf{r},t)\Psi(\mathbf{r},t), \quad (4)$$

$$H(\mathbf{r},t) = H_0(\mathbf{r})+\mathbf{r}\cdot\mathbf{E}_{lp}(t)+\mathbf{r}\cdot\mathbf{E}_s(t), \quad (5)$$

$$H_0(\mathbf{r}) = -\frac{1}{2}\nabla_{\mathbf{r}}^2+V(\mathbf{r}), \quad (6)$$

where $r = x,y$, $V(\mathbf{r})$ is the two center Coulomb potential, and the matter-field interaction is treated in the length gauge, is solved numerically by a three-point difference combined with higher-order split-operator methods [26,27]. The time step is

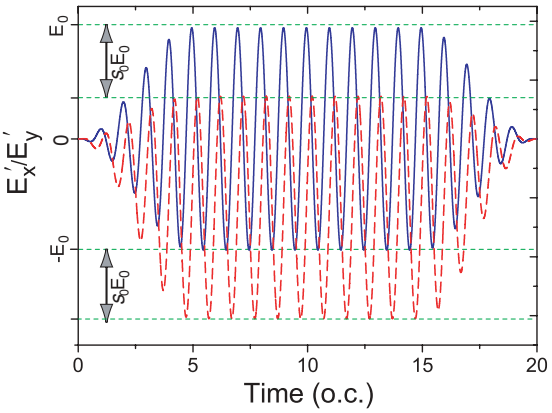


FIG. 2. (Color online) Total fields $E'_x$ and $E'_y$ obtained with a circularly polarized laser pulse $\mathbf{E}_{lp}$ and a static electric field $\mathbf{E}_s$. The field $x$ and $y$ components are, respectively, $E'_x = E_x = E_0 f(t)\cos(\omega t + \phi)$ (blue solid lines) and $E'_y = E_y + E_s = E_0 f(t)\sin(\omega t + \phi) - s_0 f(t)$ (red dashed lines), where the pulse CEP $\phi = 0.1\pi$.

fixed at $\Delta t = 0.01$ a.u. (1 a.u. = 24 asec). The total external field is written as

$$\begin{aligned}\mathbf{E}(t) &= \mathbf{E}_{lp}(t) + \mathbf{E}_s(t) = \hat{e}_x E'_x(t) + \hat{e}_y E'_y(t) \\ &= \hat{e}_x E_0 f(t)\cos(\omega_0 t) + \hat{e}_y E_0 f(t)\sin(\omega_0 t) \\ &\quad + \hat{e}_y s_0 f(t),\end{aligned} \tag{7}$$

where the static field $E_s = -s_0 f(t)$ is oriented parallel to the $y$ axis, and $f(t)$ is the field envelope. The laser duration is $T_p = n_{cy}\tau$ for an $n_{cy}$ pulse, where one optical cycle (o.c.) $\tau = 2\pi/\omega_0$. In the subsequent applications, $n_{cy} = 20$ is chosen. We use a trapezoidal pulse envelope $f(t)$ with five optical cycles at a smooth turn on, ten optical cycles at full strength, and five optical cycles at turn off, as shown in Fig. 2. To prevent unphysical effects due to the reflection of the wave packet from the boundary, a "mask function" with the following form is applied

$$g(t) = \begin{cases} 1, & r < r_0, \\ \cos^{1/8}\left[\frac{\pi(r-r_0)}{2r_{\rm abs}}\right], & r_0 \leqslant r \leqslant r_{\rm max}. \end{cases} \tag{8}$$

For all results reported here, we set the "absorber" domain $r_{\rm abs} = r_{\rm max} - r_0 = 32$ a.u. and $r_{\rm max} = 256$ a.u.. This allows us to recapture all recolliding electrons since the maximum displacement along any direction is $\alpha_m = E_0/\omega_0^2 \ll r_{\rm max}$. The MHOHG power spectrum $P_r(\omega)$ is obtained from the absolute square of the Fourier transforms (FTs) of the dipole acceleration $\langle \ddot{r}(t)\rangle$:

$$P_r(\omega) = |a_r(\omega)|^2 = \left|\int \exp(-i\omega t)\langle \ddot{r}(t)\rangle dt\right|^2, \tag{9}$$

with the laser induced electron acceleration obtained from the exact time-dependent electron wave function $\Psi(\mathbf{r},t)$:

$$\langle \ddot{r}(t)\rangle = \langle \Psi(\mathbf{r},t)\,|-\partial H(\mathbf{r})/\partial \mathbf{r}|\,\Psi(\mathbf{r},t)\rangle. \tag{10}$$

For the 20 optical cycles pulse used here, the MHOHG spectra calculated from the FTs of dipole moment, velocity, and acceleration forms give identical results [28], thus satisfying gauge invariance.

The time profile analysis [29] provides the recollision time $t_c$ of the ionized electron as it is guided by the time-dependent field $\mathbf{E}(t)$ and informs us about the depopulation of the state to which the electron returns in the presence of the laser field. The time profiles of harmonics are obtained via a Gabor transform [29–31] of the time-dependent dipole acceleration which includes phase effects:

$$\ddot{d}_G(\omega,t) = \int_{-\infty}^{\infty} \exp(-i\omega t')\exp\left[-\frac{(t'-t)^2}{2\sigma_0^2}\right]\ddot{r}(t')dt'. \tag{11}$$

$\sigma_0 = 0.15$ fs is the width of the Gaussian time window in the Gabor transform and allows us to include $N \approx 10$ harmonics in the analysis. To describe the polarization properties of the emitted MHOHG spectra [32], we have also calculated the relative harmonic phase difference $\delta$. The complex integral in Eq. (9) has two $x$ and $y$ components, thus allowing us to extract the dependence of the phase difference $\delta$ between the polarized components of the emitted harmonics on the angular frequency $\omega$ [33]:

$$\delta(\omega) = |\arg[a_x(\omega)] - \arg[a_y(\omega)]|. \tag{12}$$

where $a_x(\omega)$ and $a_y(\omega)$ are the frequency dependent components of the acceleration [Eq. (9)] after a FT.

## IV. NUMERICAL RESULTS AND DISCUSSIONS

Figure 2 shows the total external fields used in the simulations, where the static electric fields $\mathbf{E}_s(t)$ are set parallel to the $y$ polarization of the circularly polarized laser field $\mathbf{E}_{lp}(t)$. We have computed MHOHG spectra for a selection of laser pulses at a fixed center wavelength $\lambda = 400$ nm (angular frequency $\omega_0 = 0.114$ a.u.) with a duration $T_p = 20\tau = 26.7$ fs. The numerical results for $x$-aligned $H_2^+$ molecular ions are obtained from the solutions of the corresponding 2D TDSE [Eqs. (4), (5), and (6)]. For all calculations, the internuclear distance is always kept at the equilibrium position $R_e = 2.0$ a.u., and the laser intensities are fixed at $I_0 = 5 \times 10^{14}$ W/cm$^2$ ($E_0 = 0.1194$ a.u. $= 6.14 \times 10^8$ V/cm).

We first consider the case of the electron recollision with the parent ion to induce maximum kinetic energy $K_e(t_c) = 9.05U_p$. The parameters of the laser and static electric field are predicted by the classical recollision model in Eqs. (2) and (3). Figure 3 shows the results with pulse intensity $I_0 = 5 \times 10^{14}$ W/cm$^2$ ($E_0 = 0.1194$ a.u.), CEP $\phi = 0.016\pi$ ($n = 0$), and static electric field strength $s_0 = 0.414E_0 = 0.04943$ a.u. ($2.54 \times 10^8$ V/cm). The simple classical model has been shown to apply also to nonzero initial velocities; however, the maximum energy can only be obtained with zero initial velocity [8]. The corresponding Keldysh parameter is $\gamma \approx 1$, where tunneling ionization processes occur. The parameter $\gamma^2$ corresponds to ratio of the energy of ionization, $I_p$, and the kinetic energy acquired in the circularly polarized laser field, $2U'_p$, with the ponderomotive energy of an electron defined as $U'_p = (E_x^2 + E_y^2)/4\omega_0^2$. In the circularly polarized laser and static electric field, the electron kinetic energy is the sum of the energies in the circularly polarized laser pulse and static field individually, and the latter $\langle (s_0 t)^2/2\rangle$ depends on the field duration time

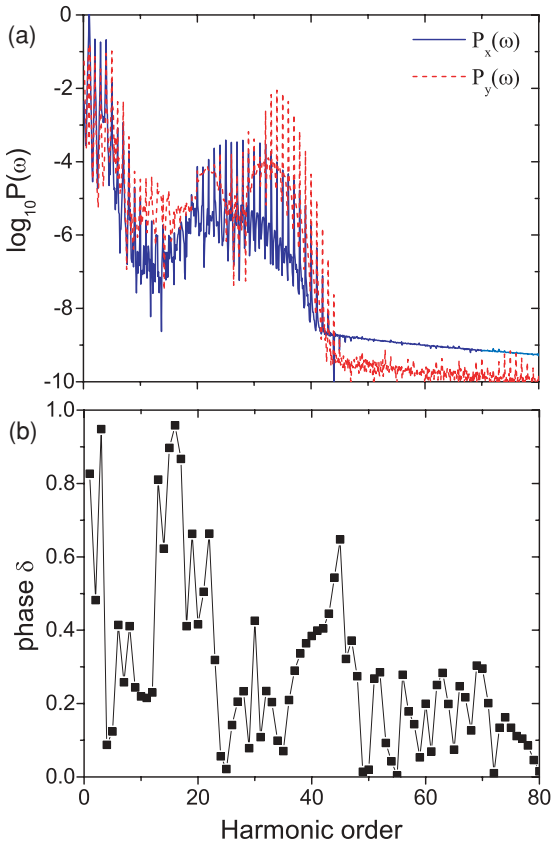


FIG. 3. (Color online) (a) $x$ and $y$ components of MHOHG spectra and (b) corresponding phase differences $\delta$ [Eq. (12)] for $H_2^+$ with the field shown in Fig. 2. The ionizing circularly polarized laser pulses have wavelength $\lambda = 400$ nm ($\omega_0 = 0.114$ a.u.), intensity $I_0 = 5 \times 10^{14}$ W/cm$^2$ ($E_0 = 0.1194$ a.u.), and pulse CEP $\phi = 0.016\pi$. The corresponding static electric field strength $s_0 = 0.414E_0 = 0.04943$ a.u. ($2.54 \times 10^8$ V/cm). The harmonic cutoff order $N_m \approx (I_p + 9.05U_p)/\omega_0 = 33$.

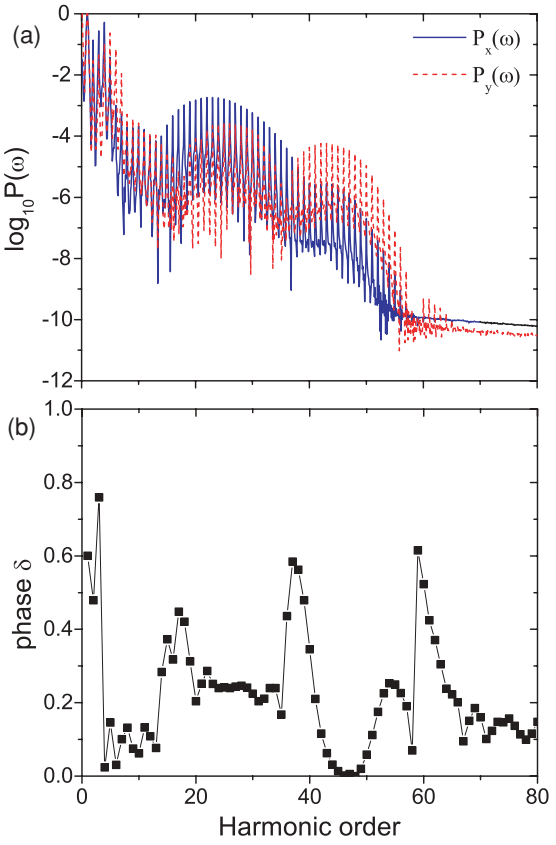


FIG. 4. (Color online) (a) $x$ and $y$ components of MHOHG spectra and (b) corresponding phase difference $\delta$ [Eq. (12)] for $H_2^+$ with the field shown in Fig. 2. The ionizing circularly polarized laser pulses have wavelength $\lambda = 400$ nm ($\omega_0 = 0.114$), intensity $I_0 = 5 \times 10^{14}$ W/cm$^2$ ($E_0 = 0.1194$ a.u.), and pulse CEP $\phi = 0.1\pi$. The corresponding static electric field strength $s_0 = 0.617E_0 = 0.07367$ a.u. ($3.8 \times 10^8$ V/cm). The harmonic cutoff order $N_m \approx (I_p + 6.34U_p)/\omega_0 = 26$.

In Fig. 3(a), we report the MHOHG spectra with laser pulse CEP $\phi = 0.016\pi$ ($n = 0$) with a plateau between harmonic orders $N = 20$ and 35 with a cutoff around order 32 obtained for both $x$ and $y$ components. The numerical results are in excellent agreement with the results $N_m = (I_p + 9.05U_p)/\omega_0$ predicted by the classical recollision model [Eqs. (2) and (3)]. With a circularly polarized laser pulse, we emphasize that for equilibrium $H_2^+$, no harmonic is appreciably produced and observed numerically, and none for the H atom since the ionized electron never collides with the parent ion. Under the influence of the static electric field, the ionized electron can come back to recollide with parent ions, thus resulting in efficient harmonic spectra. In Fig. 3(a) in the cutoff region, the harmonic signal intensity of the $y$ component is about three orders stronger than that of the $x$ component. In Eq. (2) at recollision time $t_c$, the corresponding velocity $\dot{y}(t_c) > \dot{x}(t_c)$ ($K_{ey} > K_{ex}$). As a result, more photons contribute to the $y$ component harmonics. Due to this asymmetry, both odd and even order harmonics are now obtained in the MHOHG spectra.

In Fig. 3(b), we show the phase differences $\delta$ between the MHOHG $x$ and $y$ components as a function of the harmonic order $N$. We note that the harmonic phase difference $\delta$ is very sensitive to the harmonic order $N$, indicating different processes for the generation of harmonics. Near the cutoff region $N_m = 32$, where the MHOHG is produced by the recollision of the electron with the parent ion, the phase differences $\delta$ are close to 0. The calculation shows that elliptically polarized MHOHG spectra are generated in the fields.

A calculation for the generation of MHOHG spectra by an intense circularly polarized laser and static electric field, similar to that shown in Fig. 3, but with stronger static electric field strength $s_0 = 0.617E_0 = 0.07367$ a.u. ($3.8 \times 10^8$ V/cm), is shown in Fig. 4. Here, the CEP $\phi$ of the circularly polarized laser pulse in Eq. (1) is taken as $\phi = 0.1\pi$ ($n = 0$). From the classical model in Eqs. (2) and (3), the kinetic energies $K_{ex} = K_{ey} = 3.17U_p$ and total $K_e = 6.34U_p$. Under such a laser and static electric field, in Fig. 4(a) for both $x$ and $y$ components of the MHOHG spectra, a longer plateau between harmonic orders 10 and 35 with cutoff around harmonic order $N_m = (I_p + 6.34U_p)/\omega_0 = 26$ is obtained. However, we see that in the cutoff region, the harmonic signal intensity of the $x$ component is about one order stronger than that of the $y$ component. This is inconsistent with the kinetic energy of the return electron predicted by the classical model, due to

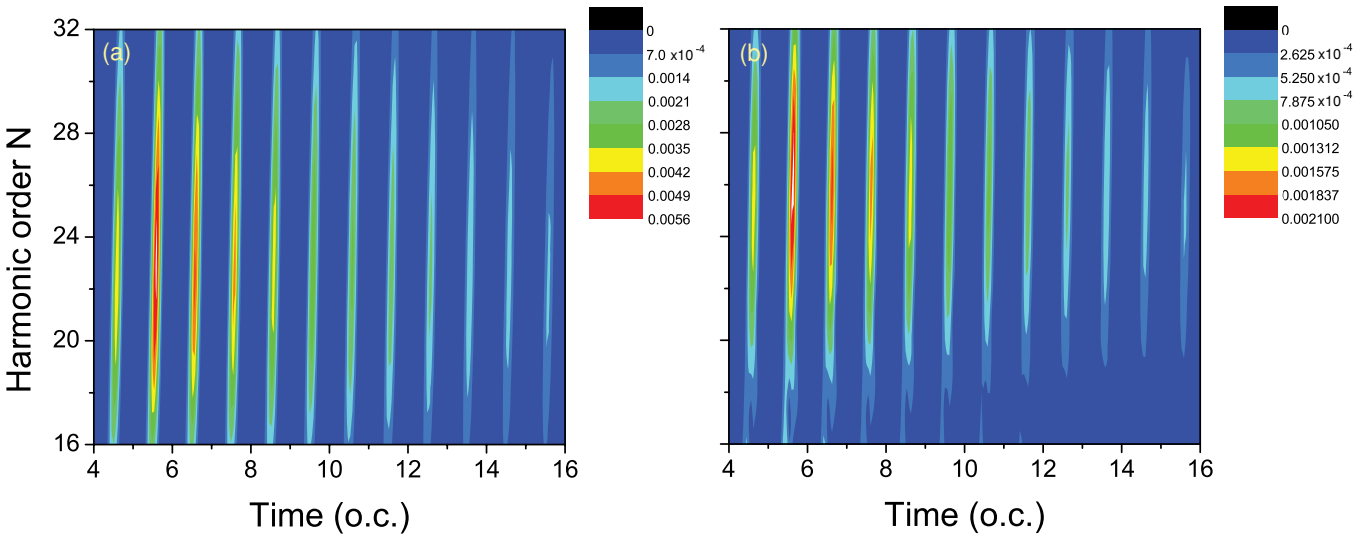


FIG. 5. (Color online)Contour plots of the time (o.c.) profile of harmonics obtained from $\ddot{d}_G(\omega,t)$ [Eq. (11)] for (a) $x$ and (b) $y$ components for $H_2^+$ in fields shown in Fig. 2, at intensity $I_0 = 5.0 \times 10^{14}$ W/cm$^2$ ($E_0 = 0.1194$ a.u.) and static field strength $s_0 = 0.617E_0 = 0.07367$ a.u. ($3.8 \times 10^8$ V/cm), corresponding to Fig. 4. Only single recollision trajectories occur at each cycle.

the neglect of the influence of the static electric field on the molecular ion ground state and Coulomb focusing [34]. In Fig. 4(b), we illustrate the MHOHG phase differences $\delta$ as a function of harmonic order $N$. Note that the phase differences $\delta$ near the cutoff region (plateau) are almost constant. Compared with the results in Fig. 3 in which the phase difference $\delta$ near the first cutoff region oscillates with harmonic order $N = 26$, a constant phase $\delta = 0.27$ is obtained in Fig. 4. These results suggest that one should adopt the case of electron recollision with kinetic energies $K_{ex} = K_{ey}$ to achieve stable MHOHG phase differences $\delta$. In Fig. 4, we further note that in the MHOHG spectra, additional plateaus, between harmonic orders 40 and 50 with maximum cutoff order about 45, beyond the first cutoff order $N_m = (I_p + 6.34U_p)/\omega_0$, are also clearly observed in $x$ and $y$ components. The second plateaus are weaker than the first ones. Moreover, in the second plateau, the intensity of the $x$ component, however, is now weaker than that of the $y$ component, opposite to the first plateau results. Since $P_y(\omega)$ dominates, the phases $\delta$ are close to 0, and linearly polarized harmonic emission is dominant.

To clarify the recollision dynamics, we show in Fig. 5 the electron trajectories for the first plateau in Fig. 4 by performing a time series analysis [29]. The time profiles of harmonics are obtained from the dipole acceleration $\ddot{r}(t)$ [Eq. (10)] via the Gabor transform [Eq. (11)]. It is seen that for low order harmonics in the first plateau of both $x$ and $y$ components, the respective intensities $P_x(\omega)$ and $P_y(\omega)$ are mainly created by single trajectories at approximate recollision times $t_c = 0.65\tau$ (optical cycle), which are in good agreement with the classical results predicted by Eqs. (2) and (3), where the recollision time is $t_c = 1.3\pi/\omega_0 = 0.65\tau$ for $\omega_0 = 0.114$ a.u. ($\lambda = 400$ nm), thus confirming that the harmonics in the first plateau mainly result from the recollision and rescattering of the electron wave packets induced by the circularly polarized laser and static field. With single trajectories in both $x$ and $y$ components in Fig. 5, circularly polarized MHOHG spectra should be expected. However, as shown in Fig. 4(a) near the cutoff (plateau) region, the MHOHG spectrum intensity of the $x$ component is stronger than that of the $y$ component due to the influence of static field on the molecular structure and Coulomb focusing [34]. The phase differences $\delta$ in Fig. 4(a) are thus less than $\pi/2$, and elliptically polarized MHOHG spectra are obtained in the circularly polarized laser and static electric field.

In Fig. 6, we show next the circularly polarized MHOHG spectra produced by an elliptically polarized laser pulse combined with a static electric field. This will produce electrons with different velocities in the $x$ and $y$ directions as opposed to Fig. 4. We use the same laser pulse, intensity $I_0 = 5 \times 10^{14}$ W/cm$^2$ ($E_0 = 0.1194$ a.u.) and wavelength $\lambda = 400$ nm (frequency $\omega_0 = 0.114$ a.u.), as done in Fig. 4, i.e., with laser pulse CEP $\phi = 0.1\pi$. Varying the ellipticity $\epsilon = E_x/E_y$ and static field strength $s_0$, we find circularly polarized MHOHG spectra at $\epsilon = 0.67$ and $s_0 = 0.85E_0 = 0.1015$ a.u. $= 5.2 \times 10^8$ V/cm. In Fig. 6(a), near the cutoff (plateau) region, $N = 25$–$45$, the harmonics of the $x$ component are equal in intensity with those of the $y$ component and the phase differences $\delta$ are $\pi/2$ precisely [Fig. 6(b)]. Thus, using a combination of intense elliptically polarized laser and static electric fields, circularly polarized MHOHG spectra are obtained over a large range of harmonics orders [Fig. 6].

The present model focuses on laser control of electron trajectories in the plane $(x,y)$ of the molecule in order to optimize recollision with the nuclei in the plane. Thus, refocusing of these trajectories by the two nuclear centers plays an essential role, hence minimizing electron wave-packet spreading. A shorter wavelength $\lambda = 400$ nm was also chosen to decrease the recollision time from 1.8 fs (for $\lambda =$ 800 nm laser pulses) to 0.9 fs (900 asec). Of note is that the present scheme generates only single recollision trajectories at each cycle. Our calculations, therefore, suggest that these

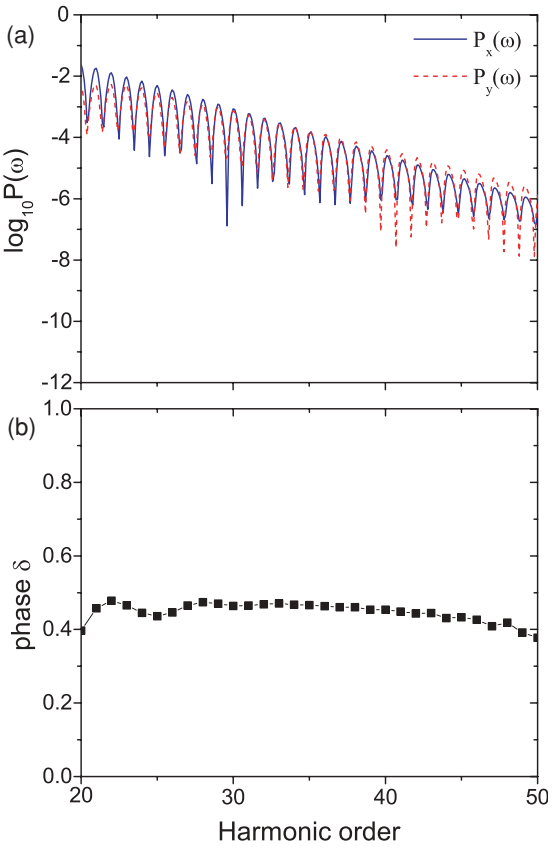


FIG. 6. (Color online) (a) $x$ and $y$ components of MHOHG spectra and (b) corresponding phase difference $\delta$ for $H_2^+$ with ionizing $\epsilon = 0.67$ elliptically polarized laser pulses, and the corresponding static electric field strength $s_0 = 0.85E_0 = 0.1015$ a.u. $= 5.2 \times 10^8$ V/cm ($E_0 = 0.1194$ a.u.).

conditions are well represented by our 2D model which has been previously shown to quantitatively describe electron dynamics by intense fields which confine and control electron motion in 2D [35].

## V. CONCLUSIONS

We present theoretical studies of the circularly polarized MHOHG spectra in the presence of intense elliptically polarized laser and static electric fields. The calculations are performed on a prealigned 2D $H_2^+$ molecular ion system by numerically solving the corresponding TDSE. A time-frequency analysis obtained via Gabor transform is employed to identify electron trajectories for the generation of the harmonic spectra. The polarization properties of MHOHG spectra are also analyzed. We first derive the recollision conditions from simple classical models for a circularly polarized laser and static electric field, thus confirming from numerical results that with particular field strengths MHOHG spectra with maximum harmonic energy $I_p + 9.05U_p$ can be obtained. In the combination of intense laser and static electric fields, these harmonics are mainly created by single recollision trajectories. Due to the kinetic energies $K_{ex}(t_c) < K_{ey}(t_c)$ of the returning electron at recollision time $t_c$, more MHOHG spectra contribute to the $y$ component, thus resulting in dominant elliptical polarization. To produce circularly polarized MHOHG spectra, we derive and calculate the results for the condition of equal kinetic energies $K_{ex} = K_{ey}$ for the recolliding electron. Because of the effects of Coulomb focusing in the ionization processes, we conclude that an elliptically polarized laser and static electric field should be used to guarantee equal harmonic amplitudes in both $x$ and $y$ components at relative phase $\delta = \pi/2$, leading to circularly polarized MHOHG. The present simulations show that static electric fields of strength $s_0 \sim 0.1$ a.u. ($5 \times 10^8$ V/cm) combined with pulses of intensity $I_0 \sim 0.12$ a.u. ($5 \times 10^{14}$ W/cm$^2$) are sufficient to control recolliding electrons for the generation of circularly polarized harmonics. Such strong static fields can be generated by low-frequency sources, such as free-electron lasers, used recently in atomic holography [36]. Furthermore, harmonic generation from ions is also now achievable with laser pulse self-compression techniques [37]. The high-order circularly polarized harmonics illustrated in Fig. 6 can be new sources for producing intense circularly polarized attosecond pulses due to the high generation efficiencies predicted by our classical and quantum simulations.

## ACKNOWLEDGMENTS

We thank Doctors X.B. Bian and S. Chelkowski for helpful discussions. The authors also thank RQCHP and Compute Canada for access to massively parallel computer clusters and CIPI (Canadian Institute for Photonic Innovations) for financial support of this research in its ultrafast science program. Furthermore, we thank the KITPC (Kavli Institute for Theoretical Physics China at the Chinese Academy of Sciences), where this paper was completed.

[1] T. Brabec and F. Krausz, Rev. Mod. Phys. **72**, 545 (2000).
[2] F. Krausz and M. Ivanov, Rev. Mod. Phys. **81**, 163 (2009).
[3] P. B. Corkum and F. Krausz, Nat. Phys. **3**, 381 (2007).
[4] A. D. Bandrauk, S. Barmaki, S. Chelkowski, and G. L. Kamta, *Progress in Ultrafast Intense Laser Science*, edited by K. Yamanouchi *et al.* (Springer, New York, 2007), Vol. III, Chap. 9.
[5] M. Lein, J. Phys. B **40**, R135 (2007).
[6] P. B. Corkum, Phys. Rev. Lett. **71**, 1994 (1993).
[7] M. Lewenstein, Ph. Balcou, M. Y. Ivanov, A. L'Huillier, and P. B. Corkum, Phys. Rev. A **49**, 2117 (1994).
[8] A. D. Bandrauk, S. Chelkowski, and S. Goudreau, J. Mod. Opt. **52**, 411 (2005).
[9] A. D. Bandrauk, S. Chelkowski, H. Yu, and E. Constant, Phys. Rev. A **56**, R2537 (1997).
[10] P. Moreno, L. Plaja, and L. Roso, Phys. Rev. A **55**, R1593 (1997).

[11] A. Bandrauk, S. Barmaki, and G. L. Kamta, Phys. Rev. Lett. **98**, 013001 (2007).
[12] M. Lein and J. M. Rost, Phys. Rev. Lett. **91**, 243901 (2003).
[13] T. Pfeifer, D. Walter, G. Gerber, M. Y. Emelin, M. Y. Ryabikin, M. D. Chernobrovtseva, and A. M. Sergeev, Phys. Rev. A **70**, 013805 (2004).
[14] K. J. Yuan and A. D. Bandrauk, Phys. Rev. A **81**, 063412 (2010).
[15] B. Wang, X. Li, and P. Fu, J. Phys. B **31**, 1961 (1998).
[16] D. B. Milošević and A. F. Starace, Laser Phys. **10**, 278 (2000).
[17] D. B. Milošević and A. F. Starace, Phys. Rev. A **60**, 3160 (1999).
[18] S. Odžak and D. B. Milošević, Phys. Rev. A **72**, 033407 (2005).
[19] R. Fischer, C. H. Keitel, R. Jung, G. Pretzler, and O. Willi, Phys. Rev. A **75**, 033401 (2007).
[20] V. D. Taranukhin, J. Opt. Soc. Am. B **21**, 419 (2004).
[21] D. B. Milošević and A. F. Starace, Phys. Rev. Lett. **81**, 5097 (1998).
[22] D. B. Milošević and A. F. Starace, Phys. Rev. A **60**, 3943 (1999).
[23] X. M. Tong and S. I. Chu, J. Phys. B **32**, 5593 (1999).
[24] Y. Xiang, Y. Niu, and S. Gong, Phys. Rev. A **79**, 053419 (2009).
[25] F. Mauger, C. Chandre, and T. Uzer, Phys. Rev. Lett. **105**, 083002 (2010).
[26] A. D. Bandrauk and H. Z. Lu, Phys. Rev. A **68**, 043408 (2003); K. J. Yuan, H. Z. Lu, and A. D. Bandrauk, *ibid.* **83**, 043418 (2011).
[27] A. D. Bandrauk and H. Shen, J. Chem. Phys. **99**, 1185 (1993).
[28] A. D. Bandrauk, S. Chelkowski, D. J. Diestler, J. Manz, and K.-J. Yuan, Phys. Rev. A **79**, 023403 (2009).
[29] P. Antoine, B. Piraux, and A. Maquet, Phys. Rev. A **51**, R1750 (1995).
[30] C. Chandre, S. Wiggins, and T. Uzer, Physica D **181**, 171 (2003).
[31] A. D. Bandrauk, S. Chelkowski, S. Kawai, and H. Z. Lu, Phys. Rev. Lett. **101**, 153901 (2008); A. D. Bandrauk, S. Chelkowski, and H. Z. Lu, J. Phys. B **42**, 075602 (2009).
[32] M. Born and E. Wolf, *Principles of Optics: Electromagnetic Theory of Propagation, Interference and Diffraction of Light*, 7th ed. (Cambridge University Press, Cambridge, 1999), Chap. I.
[33] M. Lein, N. Hay, R. Velotta, J. P. Marangos, and P. L. Knight, Phys. Rev. Lett. **88**, 183903 (2002).
[34] T. Brabec, M. Y. Ivanov, and P. B. Corkum, Phys. Rev. A **54**, R2551 (1996).
[35] J. Henkel, M. Lein, and V. Engel, Phys. Rev. A **83**, 051401(R) (2011).
[36] Y. Huismans *et al.*, Science **331**, 61 (2011).
[37] P. Arpin, T. Popmintchev, N. L. Wagner, A. L. Lytle, O. Cohen, H. C. Kapteyn, and M. M. Murnane, Phys. Rev. Lett. **103**, 143901 (2009).